(Received 12 January 2024, Accepted 9 March 2024, Scheduled 22 March 2024)

An Optimization of Subarrayed Planar Array Pattern via Fractal Structure Thinning

Ahmed Jameel Abdulqader*

College of Electronics Engineering, Ninevah University, Mosul 41002, Iraq

ABSTRACT: Dividing large planar arrays into several subarrays and then turning off some of them reduces the complexity (cost) of the system significantly. In this paper, two optimization stages for the formation of planar subarrays and the removal of some of them are proposed. The first optimization stage improves the pattern of the original planar array after dividing it into a set of rotational square and rectangular subarrays. In the second optimization stage, it works to remove some of the subarrays completely or partially, depending on new fractal structures derived from the conventional Sierpinski carpet structure. The proposed fractal-thinned planar array is based on amplitude-only excitation, i.e., the phases of the elements are set to zero. To execute the optimization steps above, a genetic algorithm (GA) is used. Some determinants are included in the optimization process to maintain the properties of the desired pattern. Simulation results showed the effectiveness of the proposed optimization method in achieving almost the same performance in both stages of optimization.

1. INTRODUCTION

Sizeable planar arrays are becoming increasingly popular in modern communication applications due to their superior sensitivity and large capacity. More radiating elements in an array mean a higher cost for the system controllers. Dividing large planar arrays into smaller subarrays is a practical way to reduce costs (i.e., complexity). The subarrayed planar array technique is a balanced trade-off between cost and system performance. To avoid generating grating periodic lobes, it is important to focus on avoiding creating regular and repeating the same structure subarrays. There are several practical ways to get rid of side lobes problems as well as to preserve other characteristics of the radiation pattern, including designing overlapping clusters using lens feeding or Butler array [1], but building these arrays is very expensive. Other methodologies have tried to solve these problems by using random polyomino subarrays [2] or random rectangular subarrays [3–5], or using the principle of rotational symmetry [6, 7], and others [8].

The use of irregular subarrays is a common choice by researchers to construct an integral beam pattern [9, 10]. Considering the complexity and cost of the system, researchers prefer to use only one or two types of planar subarrays such as T-shaped [11], or L-octimino-shaped ones [12]. However, using this type of subarray is problematic and time-consuming. Sometimes, it is impractical to precisely divide large arrays using single-shape subarrays [13], especially widely used subarrays such as square or rectangular aperture. It is easy to divide the planar array into square or rectangular subarrays, whereby simply dividing each rectangle or square into two halves by changing the direction of each half, thus this process can preserve the properties of the desired pattern. This is the idea of this connection to divide large planar arrays and break their periodicity which negatively affects the desired pattern.

After completing the process of designing the planar subarrays, it is possible that there will be a lot of small subarrays within the main aperture, and thus the array system will be somewhat complicated and expensive, in addition to generating mutual coupling between these subarrays. Here, it is important to turn off some of the subarrays without affecting the radiation characteristics of the array as a whole. This thing can be achieved by using the thinning technique. The choice of subarrays to be turned off depends on their functionality or their location within the aperture. That is, random selection can affect the system negatively. Therefore, the use of regular thinning approaches is important here, such as using fractal shapes as a thinning. The use of fractal planar array approaches gives the system the freedom to build the required patterns. The principle of fractal arrays lies in building initial arrays that contain a set of zero and non-zero elements. Thus, these arrays can be expanded to build larger fractal arrays. Many forms of fractal arrays can be built, such as Sierpinski carpet, Sierpinski gasket, and other types [14, 15]. Although fractal arrays have many advantages, they suffer from generating a high level of side lobes. It is possible to solve this problem by using several optimization methods [16–19].

In this paper, the pattern of the planar array is improved using two optimization stages based on amplitude-only excitation of elements. In the first stage, the main planar array is divided into a group of square and rectangular subarrays. During this stage, the complexity of the feeding network in terms of the number of attenuators is greatly reduced, but the radiation pattern, in this case, may suffer from high and periodic side lobes. Here,

* Corresponding author: Ahmed Jameel Abdulqader (ahmed.abdulqader@uoninevah.edu.iq).

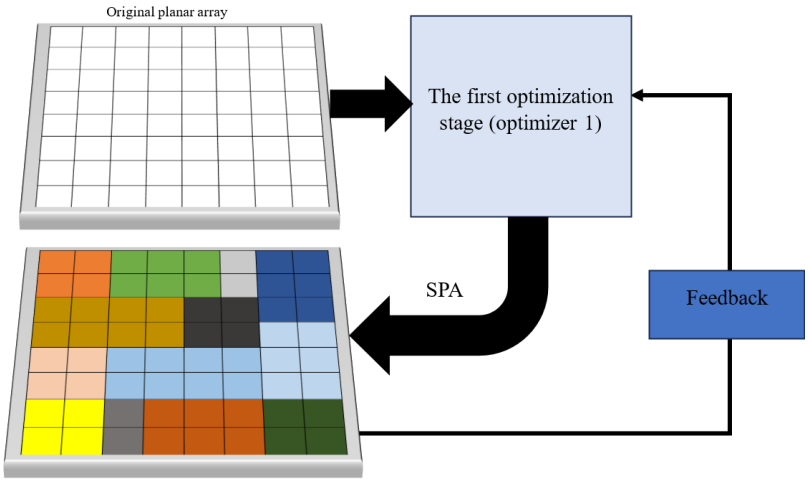

FIGURE 1. Structure of the first optimization stage.

it is necessary to reduce the number of subarrays by changing their shapes so that the square and rectangular shapes are broken. This is achieved in the second optimization stage, in which the subarrayed planar array (SPA) is fed into a fractal thinning optimizer. In this way, some subarrays will be completely or partially turned off, meaning that the SPA will contain working and non-working subarrays. In addition, the main planar array will take the form of a fractal array. By including the proposed fractal shape with the SPA, the subarrays are canceled according to the proposed fractal array decor. Both optimization stages provide good beam pattern characteristics with significant simplification of the feeding network.

2. THE METHODOLOGY OF THE PROPOSED PLANAR SUBARRAY THINNING

In this section, fully and partially fractal thinning planar subarrays are introduced highlighting their practical advantages. Clarifying the idea of this study can be divided into two stages. In this first stage, the planar array factor (PAF) is formulated by dividing the main planar array into small groups of square and rectangular subarrays, while in the second stage, the fractal array factor (FAF) is formulated to reduce the number of subarrays by eliminating them in whole or in part.

2.1. Stage 1: The Fully SPA Pattern Optimization

Consider that we have a planar array with a size $N_x \times M_y$ as shown in Figure 1. The distance between its adjacent elements in the axes x and y is fixed at 0.5λ (i.e., $d_x = d_y = 0.5$). The elements of the array will be divided into a set of small subarrays in the form of squares and rectangles equal to $S_x \times S_y$, and each subarray will contain active elements of size $n_x \times m_y$. The sizes of the small arrays are much smaller than the size of the main planar array. The PAF at angles (θ, φ) can be written as:

$$\begin{aligned} \mathrm{PAF}(\theta, \varphi) &= 4 \sum_{s_x}^{S_x/2} \sum_{s_y}^{S_y/2} E_{s_x S_y} V_{s_x s_y} \\ &\quad \sum_{n_x}^{N_x/2} \sum_{m_y}^{M_y/2} E_{n_x m_y} V_{n_x m_y} \end{aligned} \tag{1}$$

where $E_{s_x S_y}$ is the complex excitation of the subarray elements; $E_{n_x m_y}$ is the complex excitation of the individual elements of the main planar array; and $V_{s_x s_y}$ and $V_{n_x m_y}$ can be expressed as:

$$\begin{aligned} V_{s_x s_y} &= \{\cos[(s_y - 0.5) d s_y] \cos[(s_x - 0.5) d s_x]\} \\ &\quad \frac{2\pi}{\lambda} \sin\theta \cos\varphi \end{aligned} \tag{2}$$

$$\begin{aligned} V_{n_x m_y} &= \{\cos[(m_y - 0.5) d m_y] \cos[(n_x - 0.5) d n_x]\} \\ &\quad \frac{2\pi}{\lambda} \sin\theta \sin\varphi \end{aligned} \tag{3}$$

Usually, amplitude-only excitation is used when subarrays are constructed [4], so the phases of the elements in the original planar array and subarrays are set to zero. Then the amplitude excitation of the elements is set as $E_{s_x S_y} = |E_{s_x S_y}|$ and $E_{n_x m_y} = |E_{n_x m_y}|$. Here, the first-stage optimizer with $|E_{s_x S_y}|$ amplitudes are fitted in coordination with the GA to optimize the beam patterns of the square and rectangular SPAs.

2.2. Stage 2: Fractal Thinning of the SPA Pattern Optimization

The idea of thinning comes by turning on or off some subarrays (in whole or in part) with a specific decorative model by generating different new fractal structures. To implement this idea, work is done to generate a set of fractal shapes with dimensions equal to the dimensions of the main planar array. To do this, fractal array factor (FAF) is defined as follows [15, 17]:

$$\mathrm{FAF}_i(\beta) = \prod_{i-1}^{I} \mathrm{FSA}\left(\beta \alpha^{i-1}\right) \tag{4}$$

where FSA represents the expansion factor and starts from the primitive array matrix for $i = 1$. Depending on this equation, fractal shapes are formed to reduce the number of subarrays and then build the desired radiation pattern. It is possible to express FSA in the x and y axes as follows:

$$\mathrm{FSA} = \frac{1}{4} [\cos[\pi[u - u_o]] + \cos[\pi[v - v_o]]$$

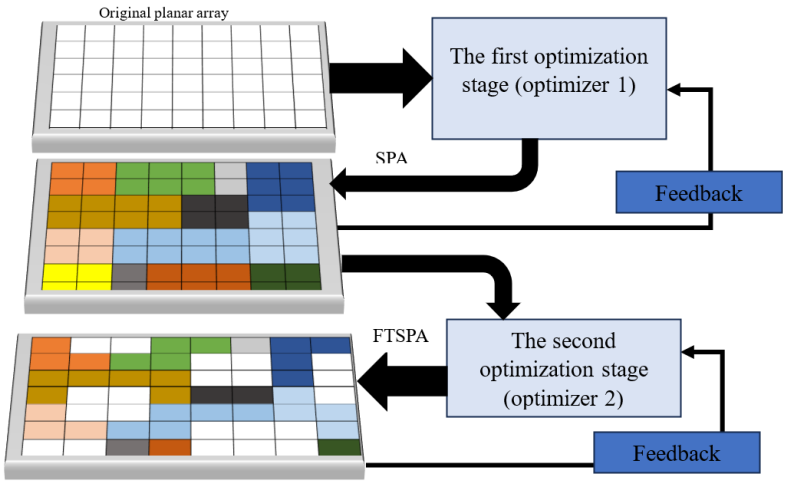

FIGURE 2. Structure of the second optimization stage.

$$+2\cos\left[\pi\left[u-u_o\right]\right]\cos\left[\pi\left[v-v_o\right]\right]\Big] \tag{5}$$

where u_o and v_o are the direction of the main beam plane, and they work in conjunction with PAF. To expand the FAF to fit the subarrayed PAF, FAF is written as:

$$\mathrm{FAF}_i\left(\beta_x,\,\beta_y\right) = \frac{1}{4^i}\prod_{i=1}^{I}\Big[\cos\left(3^{i-1}\beta_x\right)+\cos\left(3^{i-1}\beta_y\right) +2\cos\left(3^{i-1}\beta_x\right)\cos\left(3^{i-1}\beta_y\right)\Big] \tag{6}$$

Because of the nature of fractal arrays in terms of element distribution, PAF is calculated in advanced iterations, i.e., at $i > 1$. Reducing the radiating subarrays by turning off all or part of them according to the compatibility of their positions with the zero elements leads to reducing the mutual coupling between the active subarrays due to the change of distances between them.

In order to generate new fractal forms to thin the number of subarrays, first, let's start with the derivation of the traditional Sierpinski carpet elementary array matrix, and then the new fractal array matrices are derived. The primitive elemental matrix of the traditional Sierpinski carpet can be written as [21]:

$$E_{nm}^{i} = \begin{bmatrix} O & O & O \\ O & Z & O \\ O & O & O \end{bmatrix}_{i=1} \tag{7}$$

$$E_{nm}^{i+1} = \begin{bmatrix} E_{nm}^{i} & E_{nm}^{i} & E_{nm}^{i} \\ E_{nm}^{i} & Z_{nm}^{i} & E_{nm}^{i} \\ E_{nm}^{i} & E_{nm}^{i} & E_{nm}^{i} \end{bmatrix}_{i>1} \tag{8}$$

where E_{nm}^{i} and E_{nm}^{i+1} represent the primitive fractal array matrix and the next iteration fractal array matrix, respectively. O and Z represent the ones and zeros elements, respectively. The loacation of Z_{nm}^{i} in the traditional Sierpinski carpet is always in the middle of the matrix. By changing the numbers and locations of the O and Z, a new fractal shape is created. It is also possible to increase the dimensions of the primitive array matrix E_{nm}^{i} from 3×3 to 4×4 or 5×5 or 6×6 or ... etc. to produce more types of fractal shapes. By increasing the number of elements of the initial fractal array matrix, the number of possibilities for producing different fractal decorations increases. After the initial fractal array matrix and its subsequent iterations have been determined, the final subarrayed PAF can be written in coordination with the FAF as follows:

$$\mathrm{PAF}_i\left(\theta,\,\varphi\right) = E_{nm}^{i}\times4\sum_{s_x}^{S_x/2}\sum_{s_y}^{S_y/2}\left|E_{s_xS_y}\right|V_{s_xs_y} \sum_{n_x}^{N_x/2}\sum_{m_y}^{M_y/2}\left|E_{n_xm_y}\right|V_{n_xm_y} \tag{9}$$

By using fractal arrays to thin the SPA, a few subarrays will participate in shaping the final beam pattern. So, the thinning factor (TF) can be formulated as:

$$\mathrm{TF} = \frac{(N_x\times M_y)-(S_x\times S_y)_{\text{active}}}{N_x\times M_y} \tag{10}$$

$$(S_x\times S_y)_{\text{inactive}} = (N_x\times M_y)-(S_x\times S_y)_{\text{active}} \tag{11}$$

In order to maintain the characteristics of the radiation pattern as in the SPA in terms of main beamwidth and their direction, and directivity as well as the SLL, some determinants (as an objective function) are imposed on the optimization process as follows:

$$\text{Determinants} = \sum_k\left\{\mathrm{HPBW}-\mathrm{HPBW}_d\right\}^2 +\left\{\mathrm{PAF}\left(u_{\mathrm{SLL}_k},\,v_{\mathrm{SLL}_k}\right)-\mathrm{SLL}_d\right\}^2 \tag{12}$$

where k is the number of SLL angles; u_{SLL_k}, v_{SLL_k} represent the angles of the lobes on either side of the main lobe; SLL_d is the desired SLL in the SPA; and $\mathrm{HPBW}_d = \frac{1}{N_xd_x}$ or $\frac{1}{M_yd_y}$ is the desired width of the main beam on the elevation or azimuth plane. Figure 2 shows the final structure of the fractal thinned SPA (FTSPA) configuration.

The use of global optimization methods is necessary with subarrays and thinning techniques. Therefore, in this paper,

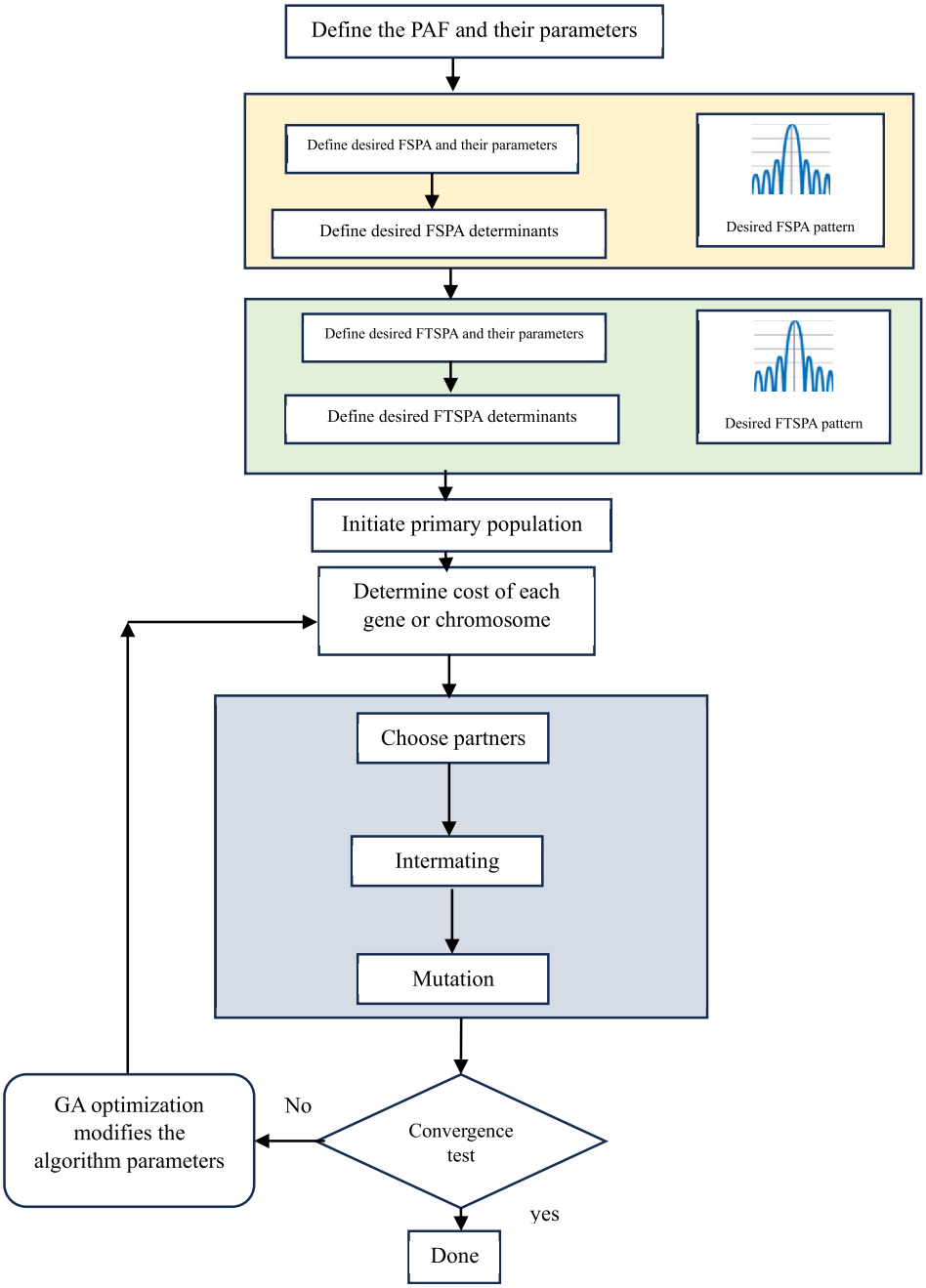

FIGURE 3. The flow chart of the optimization method.

the optimization process was assigned to the GA under the following characteristics: population number 60, a single point crossover, and 0.15 mutation rate. To clarify the optimization process more, Figure 3 shows the flowchart of the work of this algorithm.

3. SIMULATION RESULTS

In this part, several computer results are presented to show the effectiveness of the fully SPA (FSPA) and FTSPA. In all tests, a planar array with dimensions equal to the dimensions of the proposed fractal array matrix is considered. The elements of the original planar array are distributed symmetrically around the x and y axes with a spacing of 0.5λ.

In the first model, a square planar array with 36×36 elements is selected. According to the first optimization step, this array is tiled with irregular square or rectangular subarray shapes. All subarrays contain the same number of elements with different sizes. With this specification, the radiation pattern of the FSPA is improved. Then, FSPA enters the second optimizer (i.e., the second stage optimization) to turn off some subarrays completely or partially, depending on the generated fractal array matrix. Optimizer 2 initializes the proposed fractal array matrix by generating an initial fractal array matrix ($i = 1$) con-

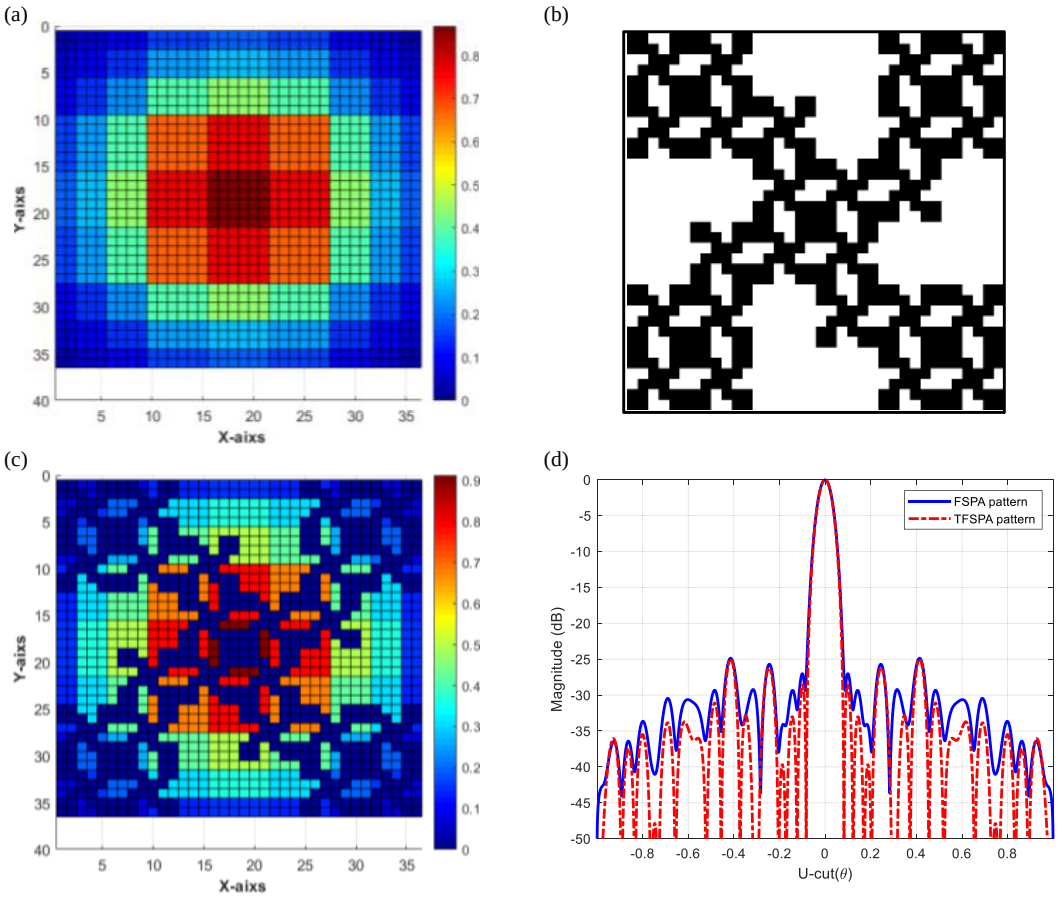

FIGURE 4. Results of the first model (a) FSPA elements distribution, (b) proposed fractal thinned structure, (c) FTSPA elements distribution, and (d) radiation pattern comparison between FSPA and FTSPA.

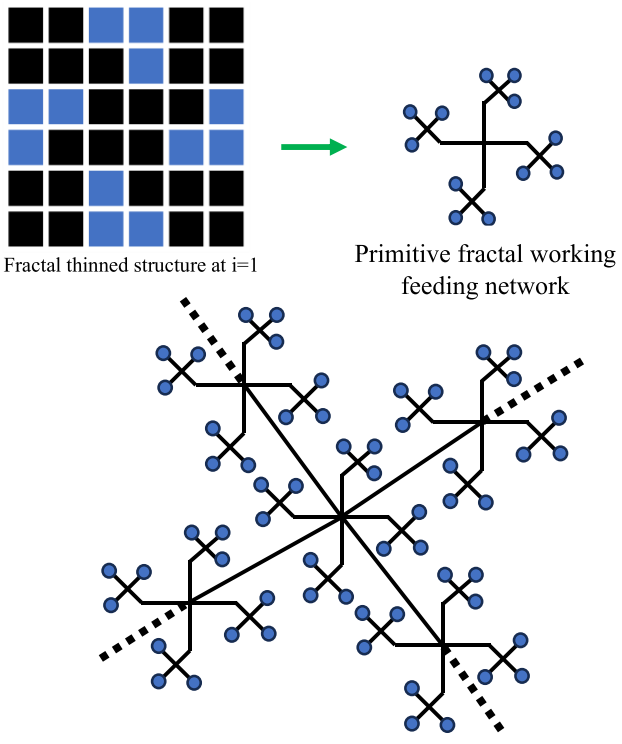

FIGURE 5. Proposed fractal working feeding network.

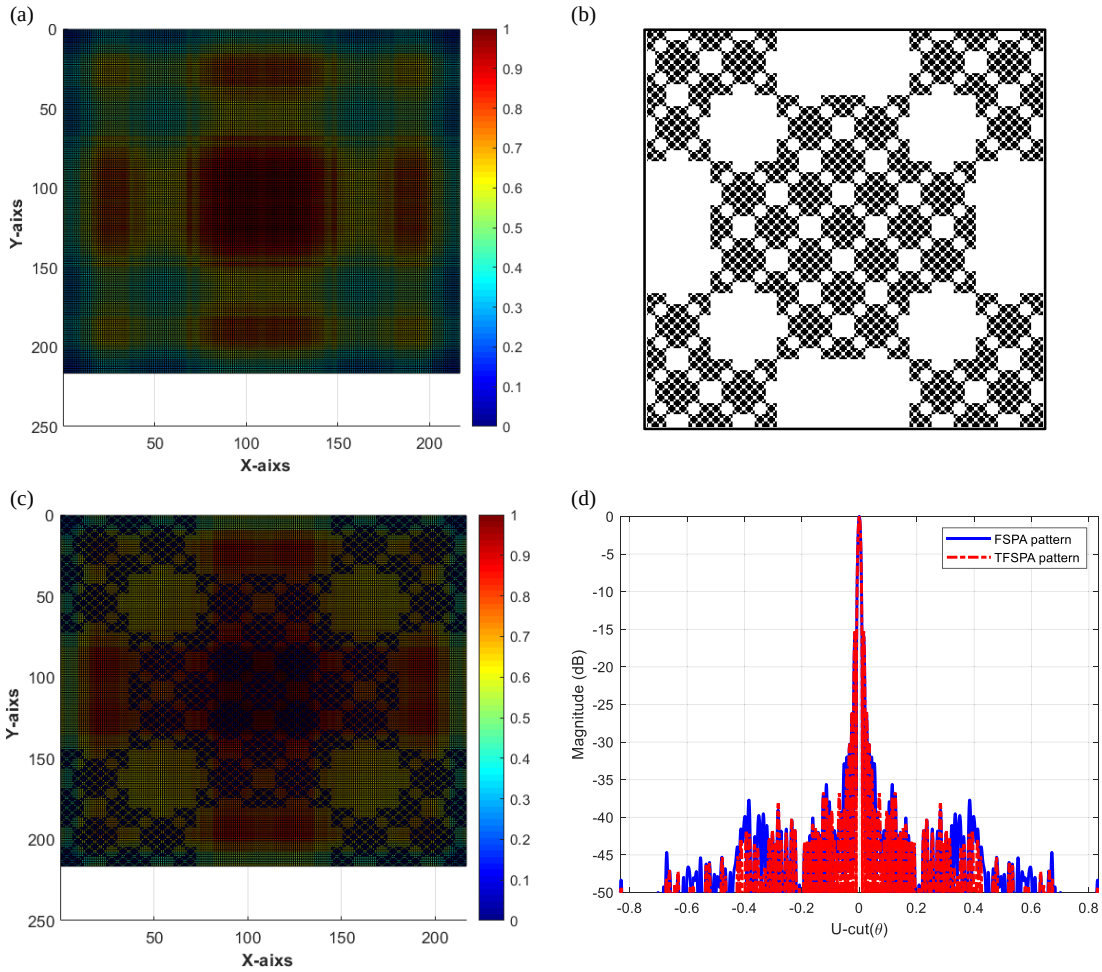

FIGURE 6. Results of the second model (a) FSPA elements distribution, (b) proposed fractal thinned structure, (c) FTSPA elements distribution, and (d) radiation pattern comparison between FSPA and FTSPA.

sisting of 6×6 elements, and then increments i greater than one to fit its size with the size of the FSPA. The assumed determinants for this model are SLL $= -25$ dB, HPBW $= 3.44$ deg with a thinning percentage of 44%. Figure 4 shows a 2D (u-cut) radiation pattern comparison between FSPA and FTSPA. From this figure, it can be seen that the two patterns have the same radiation properties under the imposed determinants. This is the goal. Also, one of the benefits of using fractal shapes as a thinning array is the great simplification of the feeding network. Therefore, the working feeding network can be designed in the form of a fractal array at $i = 1$ and then expanded to be applied to larger arrays (see Figure 5). This network feeds the active subarrays resulting from the thinning of the SPA after the second optimization stage.

In the second model, a planar array of 216×216 elements is tested. With the same scenarios followed in the first model, this model is examined. In this case, also, an initial fractal array matrix of 6×6 elements is generated, and using the expansion factor at $(i = 3)$ a thinned fractal array matrix of 216×216 is generated to match the SPA.

Figure 6 shows a 2D (u-cut) radiation pattern comparison between FSPA and FTSPA under the determinants of SLL $=$ 35 dB, HPBW $= 0.4812$ deg with a thinning percentage of 47%. From this figure, it is observed that by increasing the number of elements in the original planar array, the possibility of thinning the subarrays increases further. It is worth noting that the execution time of the algorithm in its two stages is 3 seconds (the optimization stages are done by using a core^{i7} laptop with 8 GB RAM and 2.4 GHz processors.)

Next, the performance of the thinned fractal array in terms of the relationship of SLL and HPBW with different proportions of the TF percentage has been studied in detail for the first model (see Figure 7). It is concluded from this relationship that increasing the TF percentage leads to an increase in the SLL while maintaining the main beam width. The increase in the level of the side lobes, in this case, is logical because of the decrease in the degrees of freedom of the optimizer 2. However, the important thing here is to keep the main beamwidth (HPBW) from scattering despite a significant increase in the TF.

Figure 8 shows the variation of the objective function with the number of iterations for the proposed two optimizer stages. It can be noted from this figure that the FTSPA stage requires fewer iterations to converge than FSPA stage, and this is a goal.

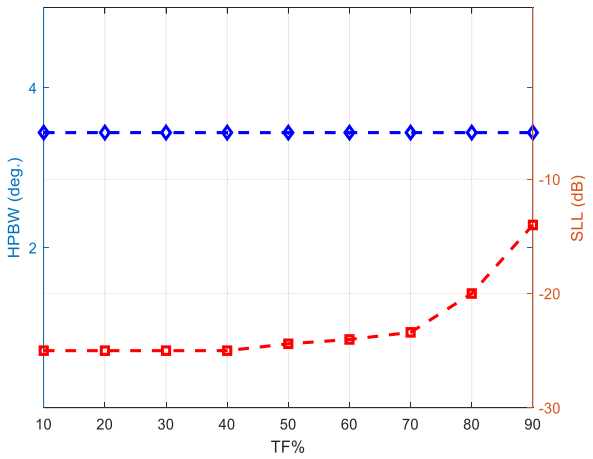

FIGURE 7. The performance of TF% with SLL and HPBW.

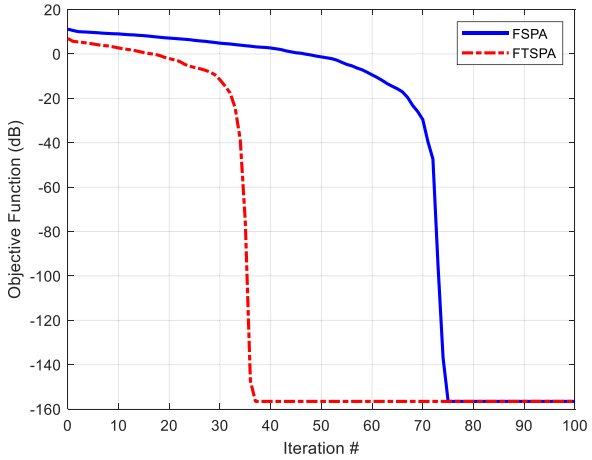

FIGURE 8. Convergence rate of FSPA and FTSPA.

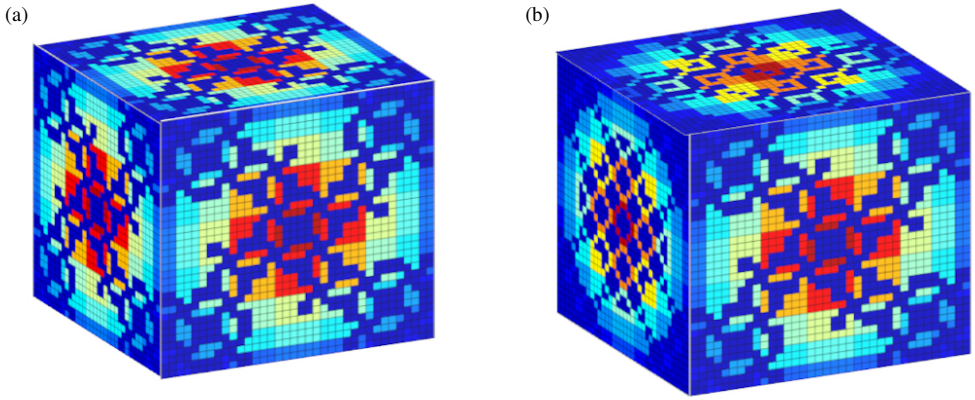

FIGURE 9. Multi-dimensional cubic planar array (a) similar faces array elements distribution, (b) different faces array elements distribution.

This gives other advantages to the proposed second optimizer stage. Finally, the proposed idea was expanded to a multi-dimensional planar array in the form of a cube with six similar faces made up of $N_x \times M_y$ elements for each face. It is also possible to build a cubic array with six different faces in terms of the fractal shape used(see Figure 9). This type of multidimensional array can be successfully applied in cube satellites such as picosatellite and Doppler radar applications.

4. CONCLUSION

It is clear from the present investigation that the desired radiation pattern characteristics can be obtained in both optimization stages in terms of low side lobes and the preservation of the HPBW. The generation of new fractal arrays derived from a conventional Sierpinski carpet as a thinning array was efficient in maintaining the required results. The obtained results by using the proposed method were a significant reduction in the complexity and cost of the feeding network from a practical point of view. In order to make the optimization process more efficient, a genetic algorithm was used. In addition, the proposed method is extended and applied to multidimensional arrays as a cube array to be suitable for working in modern applications such as satellites and radar.

ACKNOWLEDGEMENT

The author is appreciative of Ninevah University for providing the research facilities necessary to finish this study.

REFERENCES

[1] Visser, H. J., *Array and Phased Array Antenna Basics*, John Wiley & Sons, 2005.

[2] Mailloux, R. J., S. G. Santarelli, T. M. Roberts, and D. Luu, "Irregular polyomino-shaped subarrays for space-based active arrays," *International Journal of Antennas and Propagation*, Vol. 2009, 9, 2009.

[3] Wang, H., D.-G. Fang, and Y. L. Chow, "Grating lobe reduction in a phased array of limited scanning," *IEEE Transactions on Antennas and Propagation*, Vol. 56, No. 6, 1581–1586, Jun. 2008.

[4] Abdulqader, A. J., J. R. Mohammed, and Y. E. M. Ali, "Beam pattern optimization via unequal ascending clusters," *Journal of Telecommunications and Information Technology*, Vol. 1, 1–7, 2023.

[5] Mohammed, J. R., A. J. Abdulqader, and R. H. Thaher, "Array pattern recovery under amplitude excitation errors using clustered elements," *Progress In Electromagnetics Research M*, Vol. 98, 183–192, 2020.

[6] Gregory, M. D., F. A. Namin, and D. H. Werner, "Exploiting rotational symmetry for the design of ultra-wideband planar phased array layouts," *IEEE Transactions on Antennas and Propagation*, Vol. 61, No. 1, 176–184, Jan. 2013.

[7] Abdulqader, A. J., "Low complexity irregular clusters tiling through quarter region rotational symmetry," *Progress In Electromagnetics Research C*, Vol. 137, 81–92, 2023.

[8] Haupt, R. L., "Optimized weighting of uniform subarrays of unequal sizes," *IEEE Transactions on Antennas and Propagation*, Vol. 55, No. 4, 1207–1210, Apr. 2007.

[9] Isernia, T., M. D'Urso, and O. M. Bucci, "A simple idea for an effective sub-arraying of large planar sources," *IEEE Antennas and Wireless Propagation Letters*, Vol. 8, 169–172, 2009.

[10] Ahmed, J. A., R. M. Jafar, and H. T. Raad, "Unconventional and irregular clustered arrays," in *1st International Ninevah Conference on Engineering and Technology (INCET2021)*, Ninevah, Mosul, 2021.

[11] Abdulqader, A. J., J. R. Mohammed, and Y. A. Ali, "A T-shaped polyomino subarray design method for controlling sidelobe level," *Progress In Electromagnetics Research C*, Vol. 126, 243–251, 2022.

[12] Jeong, T., J. Yun, K. Oh, J. Kim, D. W. Woo, and K. C. Hwang, "Shape and weighting optimization of a subarray for an mm-Wave phased array antenna," *Applied Sciences*, Vol. 11, No. 15, 6803, 2021.

[13] Xiong, Z.-Y., Z.-H. Xu, S.-W. Chen, and S.-P. Xiao, "Subarray partition in array antenna based on the algorithm X," *IEEE Antennas and Wireless Propagation Letters*, Vol. 12, 906–909, 2013.

[14] El-Khamy, S. E., H. F. El-Sayed, and A. S. Eltrass, "A new adaptive beamforming of multiband fractal antenna array in strong-jamming environment," *Wireless Personal Communications*, Vol. 126, No. 1, 285–304, Sep. 2022.

[15] Werner, D. H., R. L. Haupt, and P. L. Werner, "Fractal antenna engineering: The theory and design of fractal antenna arrays," *IEEE Antennas and Propagation Magazine*, Vol. 41, No. 5, 37–59, Oct. 1999.

[16] Abdulqader, A. J., J. R. Mohammed, and R. H. Thaher, "Phase-only nulling with limited number of controllable elements," *Progress In Electromagnetics Research C*, Vol. 99, 167–178, 2020.

[17] Abdulqader, A. J. and J. R. Mohammed, "New improved Sierpinski carpet structures based thinned planar array to synthesize low sidelobes radiation pattern," in *2023 International Conference on Radar, Antenna, Microwave, Electronics, and Telecommunications (ICRAMET)*, 178–183, Bandung, Indonesia, 2023.

[18] Haupt, R. L. and D. H. Werner, *Genetic Algorithms in Electromagnetics*, John Wiley & Sons, 2007.

[19] Brown, A. D., *Electronically Scanned Arrays MATLAB® Modeling and Simulation*, CRC Press, 2017.

[20] Karmakar, A., R. Ghatak, R. K. Mishra, and D. R. Poddar, "Sierpinski carpet fractal-based planar array optimization based on differential evolution algorithm," *Journal of Electromagnetic Waves and Applications*, Vol. 29, No. 2, 247–260, Jan. 2015.